Effect of Pulmonary Surfactant Protein SP-B on the Micro- and Nanostructure of Phospholipid Films

Antonio Cruz,* Luis Vázquez,† Marisela Vélez,‡ and Jesús Pérez-Gil*

*Departamento de Bioquímica, Facultad de Biología, Universidad Complutense, 28040 Madrid, Spain; †Instituto de Ciencia de Materiales de Madrid (CSIC), Campus de la Universidad Autónoma de Madrid, 28049 Madrid, Spain; and ‡Instituto Universitario de Ciencia de Materiales "de Madrid Cabrera," Universidad Autónoma de Madrid, Spain

ABSTRACT Monolayers of dipalmitoylphosphatidylcholine (DPPC) and DPPC/dipalmitoylphosphatidylglycerol (DPPG) (7:3, w/w) in the absence or in the presence of 2, 5, 10, or 20 weight percent of porcine surfactant protein SP-B were spread at the air-liquid interface of a surface balance, compressed up to surface pressures in the liquid-expanded/liquid-condensed (LE-LC) plateau of the isotherm, transferred onto mica supports, and analyzed by scanning force microscopy. In the absence of protein, the films showed micrometer-sized condensed domains with morphology and size that were analogous to those observed in situ at the air-liquid interface by epifluorescence microscopy. Scanning force microscopy permits examination of the coexisting phases at a higher resolution than previously achieved with fluorescent microscopy. Both LE and LC regions of DPPC films were heterogeneous in nature. LC microdomains contained numerous expanded-like islands whereas regions apparently liquid-expanded were covered by a condensed-like framework of interconnected nanodomains. Presence of increasing amounts of pulmonary surfactant protein SP-B affected the distribution of the LE and LC regions of DPPC and DPPC/DPPG films both at the microscopic and the nanoscopic level. The condensed microdomains became more numerous but their size decreased, resulting in an overall reduction of the amount of total LC phase in both DPPC and DPPC/DPPG films. At the nanoscopic level, SP-B also caused a marked reduction of the size of the condensed-like nanodomains in the LE phase and an increase in the length of the LE/LC interface. SP-B promotes a fine nanoscopic framework of lipid and lipid-protein nanodomains that is associated with a substantial mechanical resistance to film deformation and rupture as observed during film transference and manipulation. The effect of SP-B on the nanoscopic structure of the lipid films was greater in DPPC/DPPG than in pure DPPC films, indicating additional contributions of electrostatic lipid-protein interactions. The alterations of the nanoscopic structures of phospholipid films by SP-B provide the structural framework for the protein simultaneously sustaining structural stability as well as dynamical flexibility in surfactant films at the extreme conditions imposed by the respiratory mechanics. SP-B also formed segregated two-dimensional clusters that were associated with the boundaries between LC microdomains and the LE regions of DPPC and DPPC/DPPG films. The presence of these clusters at protein-to-lipid proportions above 2% by weight suggests that the concentration of SP-B in the surfactant lipid-protein complexes may be close to the solubility limit of the protein in the lipid films.

INTRODUCTION

Pulmonary surfactant protein SP-B is absolutely required for respiratory function (Weaver and Conkright, 2001). Congenital lack of SP-B results in lethal neonatal respiratory distress syndrome in mice and humans (Clark et al., 1995; Nogee et al., 1994). Protein SP-B is a component of pulmonary surfactant, a lipid/protein complex secreted by the alveolar epithelium of lungs. Pulmonary surfactant reduces the surface tension of the air-liquid interface and prevents collapse of alveoli at end-expiration (Goerke, 1998; Perez-Gil, 2002). Dipalmitoylphosphatidylcholine (DPPC) is the main phospholipid in surfactant and also the main surface active constituent. DPPC monolayers reduce surface tension close to 0 mN/m at an air-liquid interface. Pulmonary surfactant also contains anionic phospholipids, like phosphatidylglycerol (PG), which has been proposed to participate in selective lipid-protein interactions (Perez-Gil et al., 1995; Takamoto et al., 2001). Supplementation with exogenous surfactant preparations is now a common practice for the treatment of severe respiratory distress due to surfactant insufficiencies, such as those occurring in premature babies (Frerking et al., 2001). Therapeutic surfactant preparations routinely used at present in respiratory medicine are of animal origin and contain DPPC, PG, and SP-B. However, development of new human-like artificial surfactants is a major objective of the research in the field, and new preparations are now under development including peptide analogs of human SP-B (Johansson et al., 2001). Despite all this, we are still far from understanding the molecular mechanisms and the structure-function relationships of lipids and proteins in pulmonary surfactant.

Native SP-B is a dimer of two 79-amino-acid polypeptides, cationic in nature, and so hydrophobic that it co-isolates with phospholipids in chloroform/methanol extracts of surfactant material (Hawgood et al., 1998). SP-B is produced in lung type II pneumocytes as a 381-amino-acid precursor. Processing of the SP-B precursor is coupled with the assembly of pulmonary surfactant in packed bilayers in lamellar bodies (Weaver, 1998). The three-dimensional structure of SP-B has not been determined, but different

Submitted February 26, 2003, and accepted for publication September 16, 2003.

Address reprint requests to Jesús Pérez-Gil, Dept. Bioquímica, Fac. Biología, Universidad Complutense de Madrid, 28040 Madrid, Spain. Tel.: 34-91-3944994; Fax: 34-91-3944672; E-mail: jpg@bbm1.ucm.es.

0006-3495/04/01/308/13 $2.00

models suggest that its conformation could be dominated by several amphipathic α-helices (Cruz et al., 1995), like that of the homologous proteins saposins and NK-lysin (Liepinsh et al., 1997). SP-B locates superficially when reconstituted in phospholipid bilayers, with its helices oriented parallel to the plane of the bilayers (Vandenbussche et al., 1992), producing just limited perturbations on the packing of phospholipid acyl chains (Cruz et al., 1997, 1998; Morrow et al., 1993; Perez-Gil et al., 1995). These perturbations, however, are enough to produce destabilization of the bilayer and to promote phenomena such as fusion, content leakage, or lipid exchange for phospholipid vesicles (Hawgood et al., 1998; Perez-Gil, 2001).

Lipid-protein interactions of SP-B may induce rapid transfer of surfactant surface-active molecules into the air-liquid interface (Ross et al., 2002; Schram and Hall, 2001; Cruz et al., 2000), and may modulate the stability and the dynamic behavior of the interfacial surfactant films under continuous compression-expansion (Taneva and Keough, 1994; Ding et al., 2001; Nag et al., 1999b; Ross et al., 2002).

To understand the molecular mechanisms by which SP-B modulates surfactant film dynamics, the structure of lipid and lipid/protein interfacial films have been studied in a variety of ways. In the last decade, direct visualization of lipid and lipid-protein monolayers doped with fluorescent probes, at the air-liquid interface, has proven to be a powerful technique to obtain information about structural transitions occurring in pulmonary surfactant model films subjected to dynamic compression (Discher et al., 1996, 1999; Nag et al., 1998; Piknova et al., 2001; Knebel et al., 2002a). These studies have aided understanding of the ways in which specific surfactant proteins modulate the dynamic behavior of surfactant films, especially regarding generation and sustaining of lateral phase separations occurring in the films during compression (Perez-Gil et al., 1992; Nag et al., 1996, 1997; Ruano et al., 1998; Kramer et al., 2000; Takamoto et al., 2001; Ding et al., 2001; Cruz et al., 2000). This work has led to several models of surfactant lipid-protein interaction (Perez-Gil, 2002; Perez-Gil and Keough, 1998).

In recent years, the application of scanning force microscopy (SFM) to the study of surfactant films has provided at least one order of magnitude of higher resolution (compared with fluorescence) to study the structure of surfactant layers (Knebel et al., 2002b; Grunder et al., 1999; Nag et al., 1999a; Krol et al., 2000; Diemel et al., 2002). For SFM, the lipid-protein films must first be transferred from the air-liquid interface to flat solid supports, usually mica or graphite, before being scanned and visualized. Therefore, controls are required to ensure that the structure of the films is not perturbed during transfer. A recent report suggests that scans of interfacial films by SFM can be carried out directly at the air-liquid interface (Knebel et al., 2002b). The major advantages of SFM, in addition to the increased resolution attainable, include the characterization of three-dimensional structures and no necessity for inclusion of probes in the film. SFM has been used to detect two-to-three-dimensional transitions occurring in surfactant films compressed at high pressures (Grunder et al., 1999; Diemel et al., 2002) and the role of surfactant proteins SP-B and SP-C to promote such transitions and to maintain the association of the excluded structures with the surface film (Takamoto et al., 2001; Ding et al., 2001; Krol et al., 2000; Ross et al., 2002; Kramer et al., 2000). However, these studies have focused very little on the characterization of the liquid-expanded/liquid-condensed (LE-LC) coexistence region of the surfactant compression isotherm, on the effect of surfactant proteins to perturb the LE-LC transition and the structure of the different lipid two-dimensional phases, or on the lateral distribution of the proteins themselves. A major technical problem is to simulate the conditions at which surfactant films show LE-LC transitions in the alveolar air-liquid interface. Recent studies suggest that LE-LC phase coexistence can persist in surfactant films up to the highest pressures and even during the reversible two-to-three-dimensional structural transitions occurring at the collapse of the films (Piknova et al., 2001).

The main goal of this study is to compare and extend previous results of fluorescence studies of surfactant protein SP-B mixed with DPPC and DPPC/DPPG (Cruz et al., 2000; Nag et al., 1997) with a higher resolution structural analysis using scanning force microscopy.

MATERIALS AND METHODS

1,2-dipalmitoyl-*sn*-glycero-3-phosphocholine (DPPC), 1,2-dipalmitoyl-*sn*-glycero-3-phospho-*rac*-glycerol (DPPG), and 1-palmitoyl-2-{12-[(7-nitro-2,1,3-benzoxadiazol-4-yl)amino]dodecanoyl}phosphatidylcholine (NBD-PC) were from Avanti Polar Lipids (Pelham, AL). Chloroform and methanol solvents, HPLC grade, were from Scharlau (Barcelona, Spain). Surfactant protein SP-B was isolated from minced porcine lungs as described previously (Perez-Gil et al., 1993) by two consecutive chromatographic steps in Sephadex LH-20 and LH-60 gels (Pharmacia, Uppsala, Sweden). Protein was routinely checked for purity by SDS-PAGE and quantified by amino acid analysis. Isolated SP-B was stored in chloroform/methanol 2:1 (v/v) solutions at -20°C, until used.

DPPC and DPPC/DPPG (7:3, w/w) monolayers were prepared by spreading chloroform/methanol (3:1, v/v) solutions of the phospholipids (1 mg/mL) onto a double-distilled water subphase on a surface balance (Nima Technology, Coventry, UK). SP-B was pre-mixed with lipids in chloroform/methanol at the desired protein/lipid ratio. After waiting 10 min to allow for solvent evaporation, monolayers were compressed to the required pressure (11 mN/m in most cases) at a compression rate of 25 cm^2/min. After 10 min of equilibration, the monolayers were transferred to mica supports or glass coverslips that were previously immersed in the subphase, to form Langmuir-Blodgett (LB) films, at a transfer speed of 5 mm/min. Unless otherwise stated, the experiments were done with subphase temperatures maintained at 25 $\pm$ 1°C.

Some monolayers containing 1 mol percent of the fluorescent lipid NBD-PC were transferred as described above onto glass coverslips. Epifluorescence microscopy of the supported LB films was then performed using a Zeiss Axioplan II fluorescence microscope (Carl Zeiss, Jena, Germany) equipped with the appropriate fluorescence filters for observation of NBD-PC fluorescence (maximal fluorescence emission at 520 nm).

SFM images of monolayers transferred to mica supports were obtained with a Nanoscope IIIa scanning probe microscope (Digital Instruments, Santa Barbara, CA) operated in contact mode, using silicon nitride tips with

a force constant of 0.05 N/m. Both topography and friction images were recorded from each sample.

Digitally recorded images from both SFM and epifluorescence microscopy were quantitatively analyzed using the program Scion Image (Scion Corporation, Frederick, MD). Data shown are averaged values with standard deviation obtained after analysis of at least five different images.

RESULTS

Structure of DPPC films transferred onto a solid support

Fig. 1 illustrates that DPPC monolayers transferred to freshly-cleaved mica surfaces or glass coverslips have liquid-expanded/liquid-condensed patterns that are similar to those observed by epifluorescence in situ. Fig. 1 *a* shows the π-*A* isotherms of DPPC monolayers compressed at 25 cm^2/min, before being transferred onto glass supports at defined constant surface pressures. Fig. 1 *b* shows fluorescence pictures taken from DPPC monolayers containing 1 mol % of NBD-PC and compressed to the different indicated pressures before transfer to glass supports. At pressures between 10 and 14 mN/m, coexistence of dark probe-excluding LC domains and bright probe-containing LE background is observed. Such phase coexistence is similar to that observed for films on aqueous subphases (Cruz et al., 2000; Nag et al., 1997; Perez-Gil et al., 1992; Ruano et al., 1998). Films transferred in a similar way to freshly cleaved mica surfaces were observed under a scanning force microscope (Fig. 1 *c*) using the contact mode. The films compressed to 11 mN/m contained domains, with distributions and shapes comparable to those seen under epifluorescence microscopy. These condensed domains were distinguished in the topographical images as areas 8–13 Å higher than the average background. The liquid-condensed domains, as seen by SFM after transfer, maintain the typical kidney-bean shape observed by epifluorescence in situ on monolayers equilibrated in the LE-LC plateau of the isotherm (Mohwald, 1990; Nag et al., 1991), indicating that the transfer to the solid support does not distort the shape of the solid domains as it was at the interface.

Fig. 1 *d* compares the percent of total area in the films occupied by LC domains at different surface pressures, calculated from monolayers observed by epifluorescence in situ or from monolayers transferred to supports as LB films and observed either by epifluorescence or SFM. Only frames without fractures or scanning drift were used for quantification. All the data points define similar condensation profiles, corresponding to the LE-LC two-dimensional phase transition. Comparison of the percentage of condensed domains observed in situ and after transfer of the monolayer to a solid support indicates that in both cases the onset of nucleation starts at around 8 mN/m at 25°C and the total area of the condensed domains increases with compression up to 60 to 80% of the total film at 15–17 mN/m. Similar data have been published before from monolayers analyzed in situ at the air-liquid interface (Nag et al., 1996; Ruano et al., 1998; Perez-Gil et al., 1992; Cruz et al., 2000). This confirms that the transferred monolayers maintain the microscopic structure observed in the monolayers in situ and can therefore be used to study the films at the nanoscopic level, in the absence of fluorescent probes, by SFM.

The higher resolution of SFM compared with epifluorescence microscopy allows observation of structural details in both LC domains and LE areas which are not visible under the fluorescence microscope. Magnification images in Fig. 1 *c* show that both LE and LC phases look heterogeneous in nature. Condensed domains contain abundant holes or pores, ranging from 25 to 150 nm in diameter, whereas the areas that showed themselves as homogeneously bright under fluorescence are composed, as seen under SFM, of numerous condensed nanodomains of ~0.1–1 μm length. Topology and friction properties of these nanodomains contained into the expanded phase are undistinguishable from topological and frictional features of the large LC regions, suggesting that both come from similar molecular arrangements though seen at different scales. Numerous nanodomains appear connected with the perimeter of the large condensed micrometer-sized domains, suggesting that compression-driven growth of condensed domains could proceed via accretion of nanodomains upon reduction of the available expanded area.

Effect of SP-B on the structure of DPPC films

Fig. 2 shows the effect of the presence of percents of SP-B ranging from 2% to 20% in the distribution and morphology of LC microdomains in DPPC monolayers compressed to the LE-LC coexistence regime. The higher the concentration of protein, the higher the number of condensed microdomains are observed at pressures in the LE-LC coexistence plateau of the isotherm. This effect has been widely reported (Nag et al., 1997; Cruz et al., 2000) and attributed to perturbations induced by the protein on the phospholipid lipid packing at the nucleation sites of the domains. The increase in number, however, is associated with an overall decrease in the total area occupied by the LC domains, as quantified in Fig. 2 *a*. Condensed domains occupy 60% of the total area of the films at low protein concentration, and this percentage decreases to less than 20% in the presence of 20% SP-B.

Fig. 3 shows the effect of increasing amounts of surfactant protein SP-B on the size, distribution, and morphology of the nanodomains in the liquid-expanded phase of DPPC films. We did not detect significant effects on the height of condensed nanodomains over noncondensed areas (Fig. 3 *a*) up to protein/lipid ratios of 20% (w/w) that could reflect topological effects of the presence of the protein itself. Taking into account the area of nanodomains, as much as 90% of the total surface of DPPC films at 11 mN/m is occupied, in the absence of protein, by condensed lipid. This proportion is reduced to below 50% in the presence of 20%

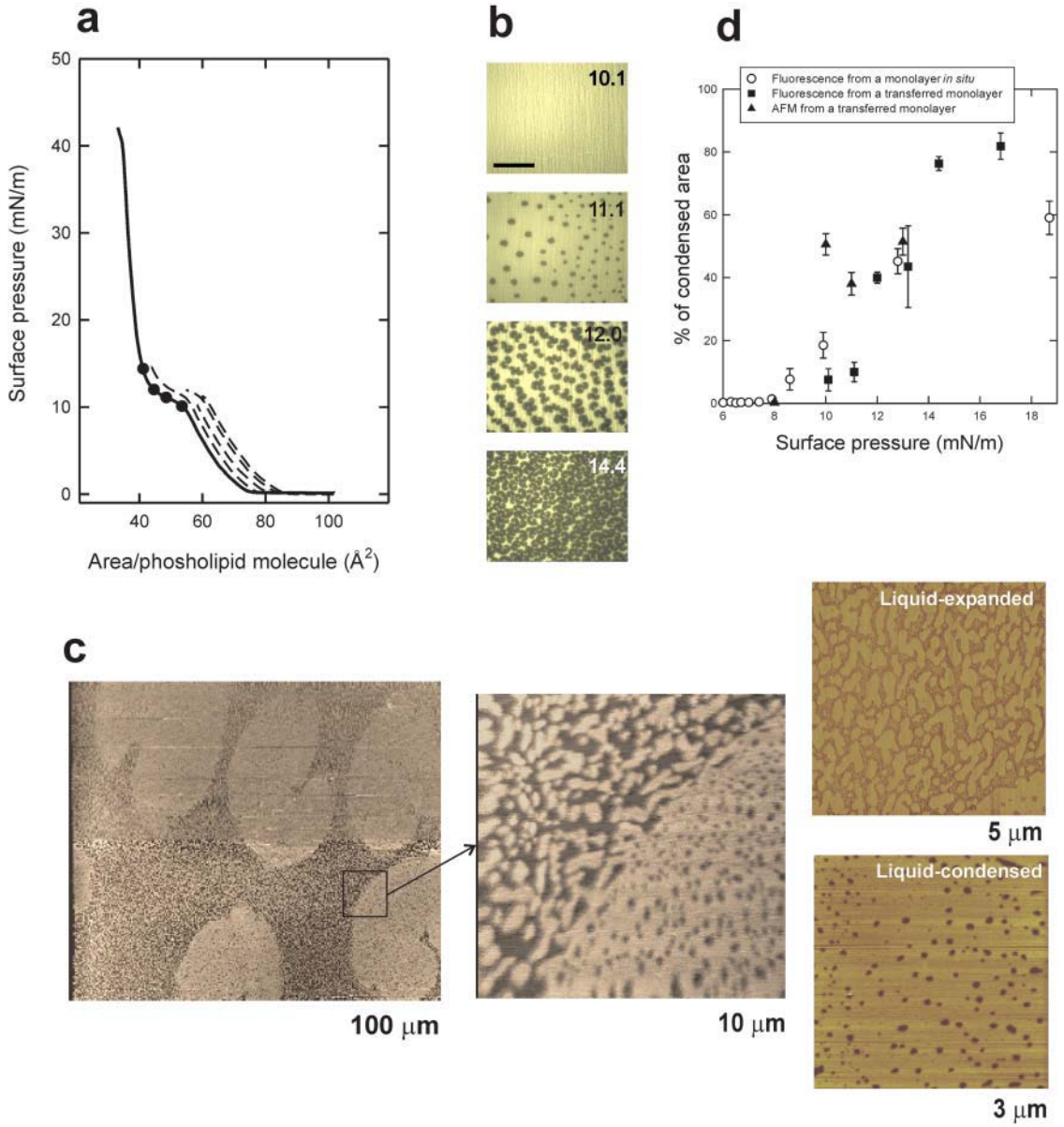

FIGURE 1 (*a*) Surface pressure versus phospholipid molecular area of a DPPC monolayer spread and compressed on the surface of a pure water interface (*continuous line*) and isotherms (*dashed lines*) of films compressed to the pressures indicated by the black dots before being transferred at constant pressure onto glass coverslips, all done at 25 ± 1°C. (*b*) Epifluorescence images (scale bar, 100 μm) of DPPC monolayers containing NBD-PC (1% mol/mol) compressed to the indicated pressures before transfer as LB films onto glass coverslips, showing dark, probe-excluding condensed domains on a bright, probe-containing liquid-expanded background. (*c*) Contact mode SFM images from a DPPC monolayer containing NBD-PC (1% mol/mol) compressed to 11 mN/m and transferred to a freshly cleaved mica surface, at different magnifications (the width size covered by each micrograph is indicated). Contrast between condensed and expanded regions comes from differences in topology or film thickness as scanned by the SFM tip. (*d*) Quantitative analysis of the percentage of the films occupied by condensed domains at different surface pressures, calculated from DPPC monolayers containing 1% (mol/mol) NBD-PC and observed in situ by epifluorescence microscopy (*open circles*, data taken from Cruz et al., 2000) or upon transfer to LB supports and observation by epifluorescence (*closed squares*) or SFM (*closed triangles*).

(w/w) SP-B. Most of this reduction in condensed areas comes from the decrease in size of the microdomains as seen in Fig. 2, with a much more limited change on the area taken by the nanodomains. At low protein concentration, 2% of SP-B, the condensed nanodomains, occupying 75% of the liquid-expanded surface, form a network that surrounds and isolates some liquid nano-areas. This overall morphology is qualitatively similar to that of the DPPC films in the absence of protein. At the highest protein/lipid ratio the condensed nanodomains are smaller, isolated, and totally surrounded by the liquid phase. The smaller nanodomains tend to have a circular shape (*red spot* in the *right bottom picture* of Fig. 3), whereas the larger ones show a branched morphology (*blue area* in the micrograph). That is, the larger domains

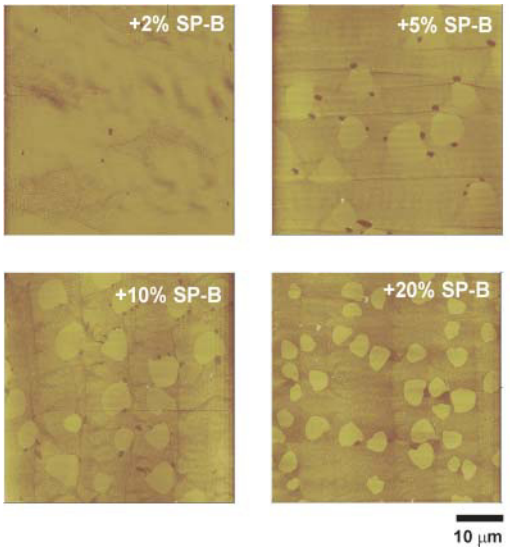

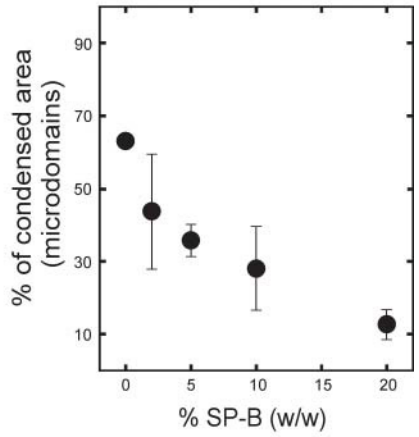

FIGURE 2 Effect of surfactant protein SP-B, at the indicated protein/lipid weight percent, on the morphology and size of large micrometer-sized condensed microdomains. Micrographs show contact mode SFM images from monolayers transferred to mica once compressed to 11 mN/m, and cover 50 μm width. (*Graph*) Effect of SP-B on the percent of total area in the films occupied by LC microdomains.

tend to increase their perimeter or liquid-condensed interface. This effect can be evaluated by plotting the ratio of total condensed area for the nanodomains over the total length of condensed/expanded interface versus the protein concentration (Fig. 3 *c*). This area/perimeter ratio undergoes a sharp decrease depending on the percent of protein present, suggesting that the protein is maximizing the condensed/expanded interface, probably by decreasing the LE-LC line tension, up to protein contents around 5% SP-B/lipid by weight. For higher amounts of protein the area/perimeter does not decrease anymore, suggesting that the lipid is at those lipid/protein percents somehow saturated with protein.

Morphological changes induced by SP-B on the nanostructure of DPPC films were associated with a substantially higher resistance of the films to undergo mechanical rupture during transference form the air/water interface to the solid supports. Pure DPPC films fractured during transfer to mica . Films containing 2% SP-B showed much fewer fractures, and those containing more than 2% SP-B were virtually unbreakable during transference under the conditions used in this study. Films containing SP-B were also remarkably more resistant to mechanical disruption by the atomic force cantilever when used at high scan force.

Effect of SP-B on the structure of DPPC/DPPG films

SP-B has been proposed to interact selectively with the fraction of PG in pulmonary surfactant (Perez-Gil et al., 1995; Takamoto et al., 2001). We therefore studied the effect of the presence of this anionic lipid species with SP-B on the structure of the films at the nanoscopic level. Fig. 4 shows the π-*A* isotherms of DPPC/DPPG (7:3, w/w) monolayers in the absence or in the presence of 2, 5, 10, or 20% SP-B by weight, and some SFM pictures of films, once compressed to 11 mN/m and transferred onto mica supports. DPPC/DPPG films have less defined LE-LC plateaus than DPPC monolayers. SP-B has similar qualitative effects on the microscopic LC domains of DPPC/DPPG films than observed in DPPC/SP-B films. The pictures of Fig. 5 illustrate that increasing amounts of SP-B also reduce the size and the area occupied by the condensed nanodomains in the LE phase of DPPC/DPPG monolayers. As observed in DPPC/SP-B films, the protein reduced the total condensation of DPPC/DPPG monolayers from 90% in the pure lipid films to ~40% in the presence of the maximal amount of protein tested. Such reduction is mostly due to melting of the large domains (as seen in Fig. 4).

The data in Figs. 2 and 4 indicate that SP-B reduces at a similar extent the area occupied by the large microdomains in the two kind of films. Fig. 6 shows that increasing SP-B concentrations reduce the area of nanodomains in the LE phase to a greater degree in DPPC/DPPG than DPPC films.

The presence of SP-B protein on DPPC/DPPG films also conferred the mechanical stability observed in SP-B/DPPC monolayers: the film did not fracture after transfer to the solid support, and it was more resistant to mechanical disruption by the atomic force cantilever when used at high scan force.

Lateral segregation of SP-B

A new feature observed in SFM micrographs of films containing SP-B is the presence of dark (low height) areas that are not observed in protein-free films. These dark spots were present in both DPPC/SP-B (Fig. 7) and DPPC/DPPG/SP-B (Fig. 8) films, and were mostly seen associated to the edges of the large LC microdomains. These dark areas were observed consistently with three different protein preparations, isolated from different batches of porcine lungs. Fig. 7 shows that the number of spots as well as the relative area occupied by the spots over the total surface increased with the percent of protein in the film. Also, the size of the spots

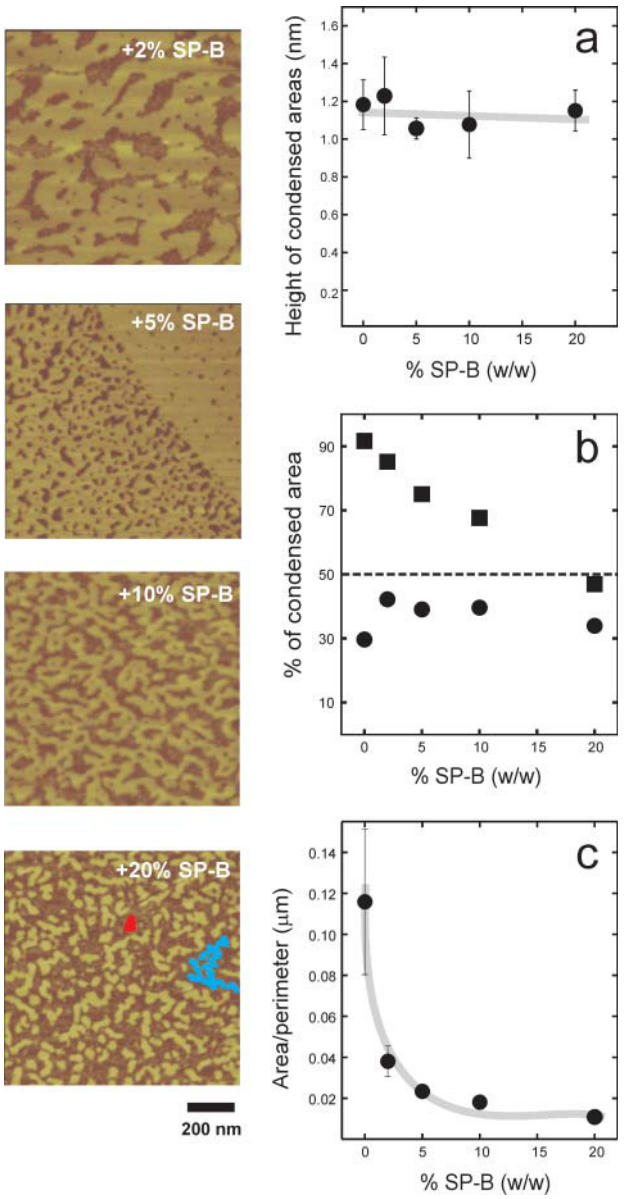

FIGURE 3 Effect of surfactant protein SP-B on the morphology of small nanometer-sized condensed nanodomains into the LE regions of DPPC films. Micrographs show SFM scans of 1 × 1 μm areas of DPPC monolayers containing the indicated protein percents by weight, compressed to 11 mN/m and transferred to mica supports. Marked are examples of small Euclidian round nanodomains (*red-colored*) and large branched fractal domains (*blue-colored*). (*a*) Effect of SP-B on the height of condensed nanodomains over expanded nano-areas of the films. (*b*) Effect of the protein on the percent of surface in the films occupied by total condensed area (*closed squares*) and small nanometer-sized condensed nanodomains (*closed circles*). (*c*) Effect of protein on the total area/perimeter ratio of the surface occupied by condensed nanodomains.

increases with the amount of protein up to 10% protein to lipid by weight. These results suggest that the dark spots are SP-B.

Interestingly, the contacts between the protein clusters and the large condensed lipid microdomains were considerably longer in the DPPG-containing films than in those made of DPPC/SP-B. Fig. 8 illustrates how in many cases the LC microdomains in DPPC/DPPG deform to extend the contact with (see microdomain embracing *cluster 1* in Fig. 8 *a* or that one almost closed around *cluster 3* in Fig. 8 *b*) and even surround (*cluster 4* in Fig. 8 *b*) the protein clusters. Some protein clusters interact simultaneously with several condensed microdomains (*cluster 2* in Fig. 8 *a* or *clusters 5* and *6* in Fig. 8 *c*). These effects are probably due to electrostatic interactions between the highly cationic SP-B aggregates and the densely packed negative charges on PG at the edges of the condensed lipid microdomains.

Fig. 9 analyzes the topological and frictional features of the different regions defined in DPPC/SP-B films. Fig. 9 *b* compares topology-based and friction-based images obtained from the same surface, sampled from a larger region (Fig. 9 *a*) that contains condensed microdomains (*area 3*), LE regions including nanodomains (*area 2*), and dark protein clusters (*area 1*). The topological image distinguishes these different regions, including a border region surrounding the dark areas with much less numerous nanodomains. The image built from the frictional properties of the film shows only two contrasted film components, indicating that the surface of the material forming the dark spots has a different chemical nature than that forming both the LE and LC regions. There is almost no contrast between condensed domains, nanodomains, and expanded phase, suggesting that the SFM tip is ''touching'' a similar material in all these regions—presumably lipid—though with different thicknesses. The image shown in Fig. 9 *c* was obtained after scratching a square hole into the dark region of the film, and then scanning with the SFM tip. The black area of the scratched square corresponds to the mica surface of the support, with some material accumulated at the limits of the surface sweep by the tip. The atomic arrangement of the mica surface could be resolved at this scratched area (not shown). Fig. 9 *c* demonstrates that the dark areas formed in the presence of protein consist of a flat material, of completely different frictional properties to lipid. A topological profile measured across the different regions of the film (Fig. 9 *d*) indicates that the flat dark regions have a homogeneous height of ~4–6 Å over the mica. The condensed regions have a real height of ~14–16 Å (relative to mica surface), for both the large condensed domains and the nanodomains of the LE phase. The area intercalated between the nanodomains as well as the area bordering the dark protein-based regions have variable heights in the range of 6–10 Å.

DISCUSSION

DPPC is the major lipid species of pulmonary surfactant and responsible for the surface active properties of this material. Investigators have believed that surfactant films at the air-liquid interface of lungs should be highly enriched in DPPC to achieve and sustain the lowest surface tensions needed to

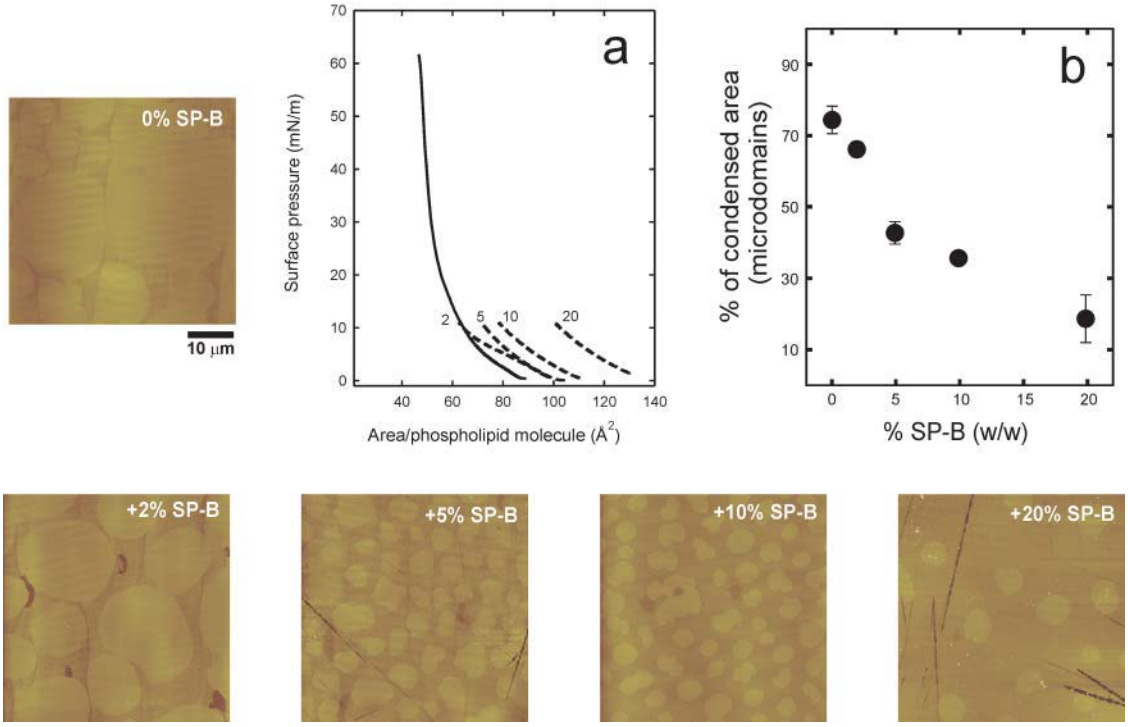

FIGURE 4 Effect of surfactant protein SP-B, at the indicated protein/lipid weight percent, on the morphology and size of large micrometer-sized condensed microdomains in DPPC/DPPG (7:3, w/w) monolayers. Micrographs show contact mode SFM images from monolayers transferred to mica once compressed to 11 mN/m, and cover 50 μm width. (*a*) π-*A* isotherms of DPPC/DPPG monolayers in the absence (*continuous line*) and in the presence (*dashed lines*) of 2, 5, 10, and 20% SP-B (w/w), compressed up to the transfer pressure (11 mN/m). (*b*) Effect of SP-B on the percent of total area in the films occupied by LC microdomains.

stabilize the respiratory epithelium (Bangham et al., 1979; Goerke and Gonzales, 1981). Different mechanisms, such as preferential squeeze-out of non-DPPC molecules (Pastrana-Rios et al., 1994) or selective insertion of DPPC (Yu and Possmayer, 1996; Veldhuizen et al., 2000), have been proposed to explain how an almost pure DPPC film is produced at the end of expiration. Newer ways of directly and indirectly observing surfactant films during compression indicated that surfactant films can sustain the lowest surface tensions by segregating DPPC in solid-condensed patches

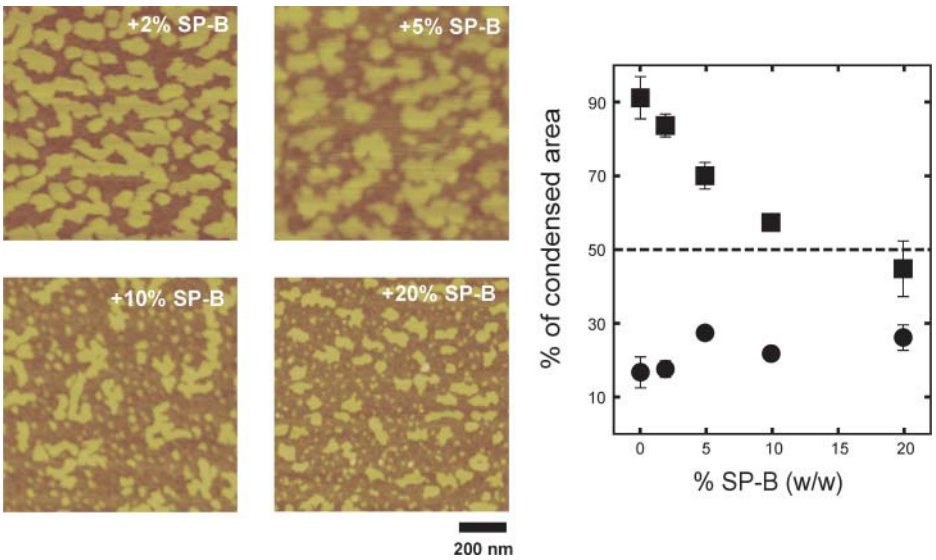

FIGURE 5 Effect of surfactant protein SP-B on the morphology of small nanometer-sized condensed nanodomains into the LE regions of DPPC/DPPG (7:3, w/w) films. Micrographs show SFM scans of 1 × 1 μm areas of monolayers containing the indicated protein percents by weight, compressed to 11 mN/m and transferred to mica supports. (*Graph*) Effect of the protein on the percent of surface in the films occupied by total condensed area (*closed squares*) and small nanometer-sized condensed nanodomains (*closed circles*).

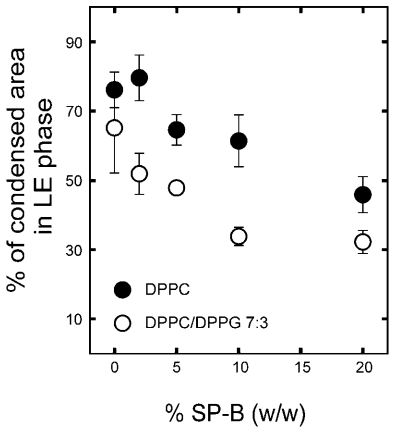

FIGURE 6 Comparative effect of SP-B on the surface occupied by condensed nanodomains into the LE regions of DPPC (*closed circles*) and DPPC/DPPG (7:3, w/w) (*open circles*) monolayers. Data points correspond to the average and standard deviation after quantitation of five different frames per sample.

(Piknova et al., 2001). Hydrophobic surfactant proteins SP-B and SP-C facilitate stability of the surface active films under the rapid compression-expansion dynamics imposed by the respiratory cycle. Selective interactions between these cationic proteins and the fraction of anionic phospholipids in pulmonary surfactant, mostly PG, are likely to be important for the biophysical action. In this study we have obtained new nanoscopic details of the effects of SP-B on the structure of DPPC and DPPC/PG interfacial films.

Micro- and nanostructure of DPPC films

The structure of pure DPPC monolayers at different states of compression has been widely studied by numerous techniques including SFM. We first confirmed, using epifluorescence microscopy, that the transfer of the monolayers to a solid support did not affect the microscopic structural details of the films and that the SFM images faithfully reproduced, both qualitative and quantitatively, what was observed with the optical microscope. The higher resolution provided by SFM images, however, revealed the existence of small domains on the submicron scale in the LE phase of DPPC, as has been previously reported (Hollars and Dunn, 1998). We confirm in this study that topological and frictional properties of these nanodomains are consistent with coexistence of both LE and LC lipids in the ''liquid-expanded'' phase that appears homogeneous under epifluorescence microscopy. Some investigators have questioned whether nanodomains are artifactual, considering possible dewetting effects or potential immobilizing contributions due to molecular adsorption to solid supports. However, more recent evidence offers both theoretical and experimental support for their existence in surfactant films in situ (Nielsen et al., 2000a,b; Reiter, 1992; Shiku and Dunn, 1998).

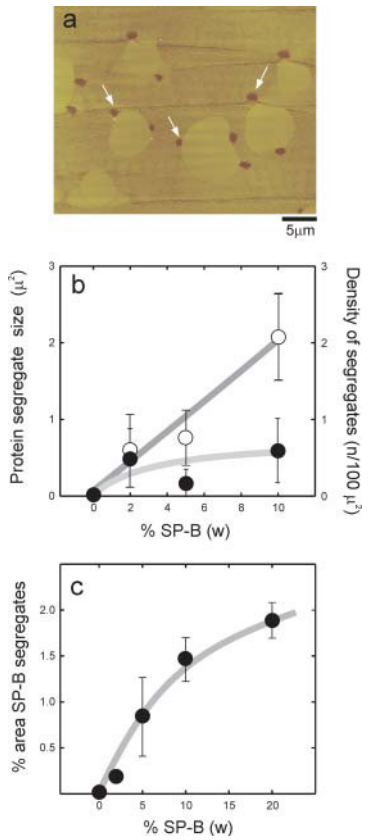

FIGURE 7 (*a*) Contact mode SFM image of a DPPC film containing 5% (w/w) surfactant protein SP-B transferred onto mica from a monolayer compressed to 11 mN/m. White arrows indicate the presence of low patches, associated at the LE/LC borders, which are not present in supported films transferred from protein-free DPPC monolayers. (*b*) Quantitative analysis of the number (*open circles*) and size (*closed circles*) and (*c*) the total area of the patches versus the amount of protein in the films.

Effects of SP-B on the nanostructure of phospholipid films

SP-B increases the number and decreases the size of the LC microdomains formed during compression of the film. This effect has been previously observed by epifluorescence microscopy (Cruz et al., 2000; Nag et al., 1997) and is similar to that caused by the other hydrophobic surfactant protein, SP-C (Perez-Gil et al., 1992; Nag et al., 1996, 1997). However, and in contrast to SP-C, SP-B did not seem previously to have important effects on the overall condensation of the lipid-protein films that occurs upon compression. That was interpreted as a consequence of a limited, potentially superficial, perturbing effect of the protein on the acyl chain packing of DPPC molecules (Nag et al., 1997; Cruz et al., 2000). Other techniques have, in fact, demonstrated that SP-B produces shallow perturbations on the packing of phospholipid molecules in bilayers (Perez-Gil et al., 1995; Morrow et al., 1993; Cruz et al., 1997, 1998). This study indicates that the effects of SP-B are more evident than previously reported, especially on the LE phase at the

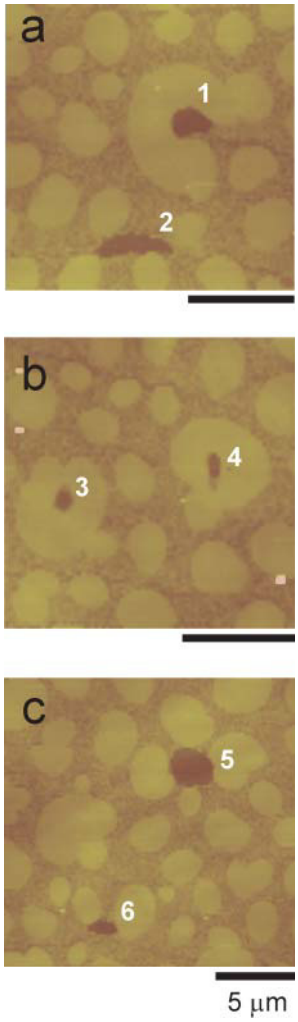

FIGURE 8 SFM images showing the presence of protein clusters (numbered *1–6*) in DPPC/DPPG (7:3, w/w) films containing 5% SP-B (w/w), compressed to 11 mN/m. Scale bars in all pictures correspond to 5 μm.

nanometer scale. The presence of SP-B produces a significant decrease on the compression-driven condensation of the films, as observed by SFM, in the absence of extrinsic fluorescent probes. A possible explanation for the apparent discrepancy between the effects of SP-B observed by epifluorescence and those detected by SFM is that in the presence of the probe required to visualize the films under fluorescence microscopy, the LE phase of DPPC is already less condensed than in the absence of the probe. The NBD-PC probe could then apparently mask part of the effects of SP-B on the lipid packing. The mechanism by which the presence of the protein affects the number and size of the liquid condensed regions is not understood. Epifluorescence microscopy has shown that SP-B preferentially partitions into LE areas in compressed DPPC monolayers (Nag et al., 1997; Cruz et al., 2000), and the protein mostly perturbs packing of DPPC or DPPG bilayers when they are in the liquid-crystalline phase (Perez-Gil et al., 1995). Thus, if its higher affinity for the LE phase keeps the protein segregated from the condensed domains, lipid-protein interactions would let SP-B sequester molecules from condensation. It is not clear, however, whether the protein would perform this action while interacting preferentially with the domain boundaries, as shown by other proteins (Ruano et al., 1998) or whether it solubilizes lipids exclusively in the pure liquid expanded phase.

If we consider the distribution of the total amount of lipid molecules in the two phases as a function of protein/lipid molar ratio, we find that the increasing presence of protein produces an overall increase in the percentage of lipid molecules in the LE phase with the concomitant decrease in the lipid molecules sequestered in the LC phase. However, micro- and nanodomains are not drained equivalently. The percentage of condensed lipid molecules in nanodomains remains constant, whereas a decrease in the number of molecules in the microdomains accounts for the total decrease in condensed phase. This behavior is similar in DPPC/SP-B and DPPC/DPPG/SP-B films. We have used the information regarding the percentage of lipids in each phase at different protein/lipid molar ratios to estimate the number of lipid molecules in the fluid phase available to each protein molecule, assuming that only lipids in the fluid phase interact with the protein. In DPPC/SP-B films, it was found that, for the low protein concentration (2% SP-B), there are around 96 lipid molecules available for each protein molecule. As the protein content increases, a saturation value of around 33 lipid molecules per protein is reached. Therefore, at protein concentrations of 5% (w/w), all lipid molecules present in the fluid phase interact with protein molecules. The number of lipid molecules per protein molecule at saturation is of the same order of magnitude as those estimated from other techniques (Shiffer et al., 1993; Perez-Gil et al., 1995). Further increases in the protein content require solubilizing lipids from the condensed phase to maintain that ratio. In DPPC/DPPG/SP-B films the amount of lipid molecules in the LE phase is larger (Fig. 5), and the ratio of lipid per protein molecule does not reach saturation at the highest amounts of protein tested. The contribution of electrostatic lipid-protein interactions in these films probably amplifies the structural effect of SP-B in a manner that could be only partly saturable.

Lipid-protein interactions of other proteins with DPPC films have shown similar effects. Increasing amounts of surfactin, a surface active lipopeptide produced by *Bacillus subtilis*, also induce a progressive decrease in the area covered by condensed lipid nanodomains into the liquid-expanded regions of DPPC films (Deleu et al., 1999). The perturbation induced by SP-B on the packing properties of DPPC is surely important to modulate the rheological properties of the surfactant films at the alveolar air-liquid interface in vivo. SP-B segregates during compression of surfactant films into protein-enriched regions where, at the

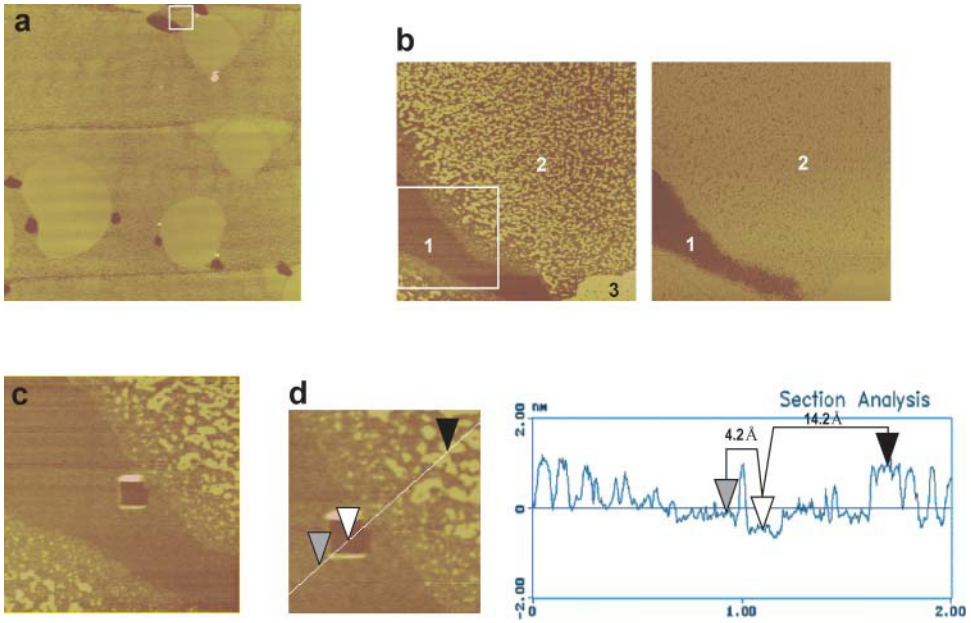

FIGURE 9 (*a*) Contact mode SFM micrograph showing topography of a 25 μm-width surface of a DPPC monolayer containing 5% (w/w) SP-B once compressed to 11 mN/m and transferred onto a mica support. (*b*) Magnification of a region centered at a single SP-B cluster, distinguishing the existence of three level surfaces (numbered *1–3*) according to topography (*left picture*) and two regions (*1–2*) according to friction (*right picture*). (*c*) Material covering the protein cluster has been scratched in a square of 200 nm to uncover the mica surface. (*d*) Topographic profile through the different regions of the DPPC/SP-B film, showing estimated heights of protein cluster and lipid nanodomains with reference to the mica surface.

high pressures achieved at the end of compression, it promotes formation of protrusions and two-to-three-dimensional transitions (Lipp et al., 1996; Krol et al., 2000). The architecture of these compressed three-dimensional phases is probably important 1), to provide enough stability to the film to reach the highest pressures—lowest surface tensions—required to avoid alveolar collapse and 2), to ensure proper respreading of the surface active material during the subsequent expansion cycle. The fine nanoscopic framework of lipid and lipid-protein nanodomains might be essential to sustain simultaneously both rheological properties of structural stability and dynamic flexibility.

Nanoscopic structure and mechanical properties of lipid and lipid-protein films

Our data indicate that the morphology of the film at the microscopic and nanoscopic scale is substantially affected by the amount of SP-B protein present and also modulated by the lipid composition of the membrane. Introduction of SP-B in DPPC or DPPC/DPPG films also prevented mechanical rupture, as observed during transfer and manipulation of the films under the scanning force microscope. We therefore suggest that the modulation by SP-B of the structure of the films, shown here at the nanoscopic level, is important to improve the rheological behavior of surfactant at the extreme physical conditions imposed by the respiratory physiology. It is well documented that the structural properties of colloidal aggregates are associated with their physical properties. Theoretical and experimentally confirmed relationships between the elastic constant and the fractal and Euclidean dimensions of gels have been found for different conditions (Shih et al., 1990). It is therefore reasonable to believe that the nanoscopic rearrangement of the film structure underlies the increased mechanical resistance rendered by the protein. In an attempt to quantify the nanoscopic changes observed, the fractal dimension, D, of the nanodomains taken individually was evaluated through the area-perimeter method. We have estimated the perimeter (P) and area (A) of each nanodomain for all the different nanodomains observed by SFM in a given sample, and the data have been plotted as a logarithmic representation of perimeter versus area. This fractal analysis of the nanodomains in DPPC and DPPC/DPPG films containing 2, 5, 10, and 20% (w/w) SP-B is presented and compared in Fig. 10. It is known (Feder, 1988) that for a set of similar objects as the nanodomains observed in the SFM images, the relationship between the perimeter and the area is $P \propto A^{D/2}$. Thus, in a logarithmic plot of P versus A, the slope of the straight regions will be equal to $D/2$. For a domain with circular or Euclidean perimeter and shape, values of D close to 1 should be obtained. In contrast, increasingly complicated perimeters and shapes should produce increasingly higher values of D. For the condensed nanodomains observed in the liquid-expanded phase of DPPC/SP-B and DPPC/DPPG/SP-B films, the P/A ratio exceeds the Euclidean one indicating that the domains tend to maximize the perimeter for a given area. In Fig. 10 *a*, the log$P$ is plotted versus log$A$ curves for the samples of DPPC containing 2 to 20% SP-B by weight. Clearly, two scaling regions can be distinguished. The first one, corresponding to small nanodomains, displays a value of D_1 in the 1.15–1.35 range, that is, a nonfractal value. The second one, in contrast, presents higher D_2 values of 1.74 for the 2% SP-B sample and around 1.9 for the rest of samples. These results imply that the smaller domains are Euclidean rather than fractal, whereas the larger ones are fractal and, therefore, the

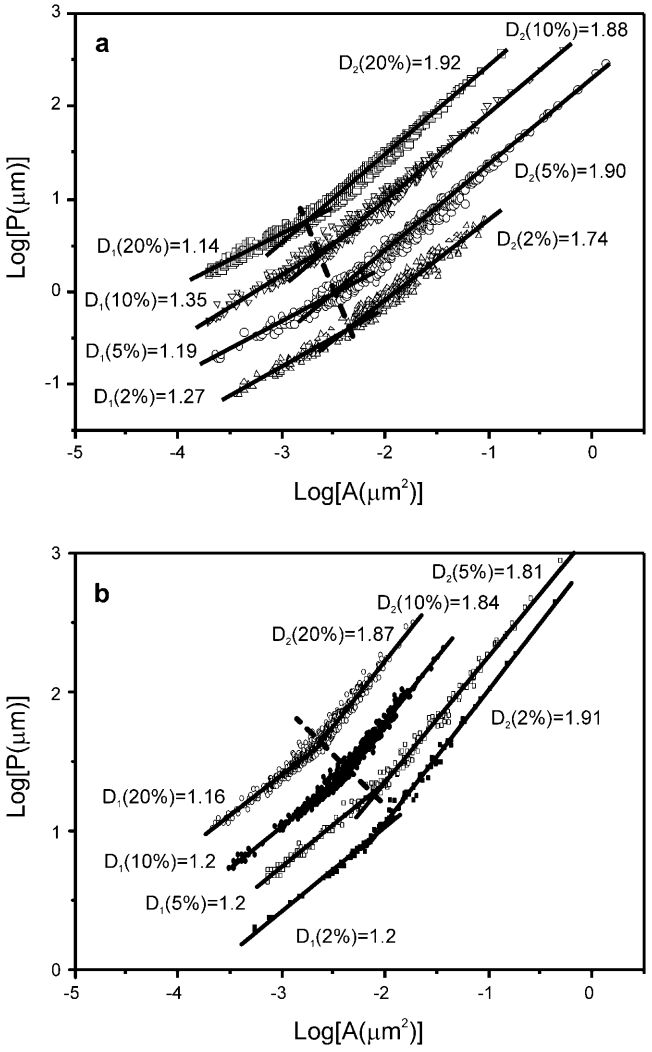

FIGURE 10 Logarithmic plot of the perimeter of single nanodomains versus their area for (*a*) DPPC and (*b*) DPPC/DPPG (7:3, w/w) films containing 2, 5, 10, and 20% SP-B by weight. Plots from films containing 5%, 10%, and 20% protein have been offset vertically to avoid overlapping and better show the lateral progressive shifting of the crossover area, which is indicated by the dashed line. For each sample, two straight lines have been drawn indicating the nonfractal (D_1) and fractal (D_2) regions of the domain perimeter.

perimeter of the domains tends to be increased. The crossover between both nonfractal and fractal regions indicates the maximal size of the nonfractal domains. Fig. 10 shows that the presence of increasing amounts of protein progressively shifts the size threshold between Euclidean and fractal nanodomains. SP-B causes a similar qualitative perturbation on the fractal profile of the liquid-expanded regions in DPPC and in DPPC/DPPG monolayers.

This analysis is capable of quantifying the structural differences induced by the presence of protein on the lipid film, which will be necessary to associate these nanostructural features with the mechanical properties of the monolayer. Measurements of the elastic properties of the surfactant films and the specific qualities of SP-B are necessary to seek correlations with the nanostructure of lipid-protein films in a more quantitative manner.

Relevance for physiological conditions

Since the conditions used in the experiments presented here are remote from those that exist in vivo, it is fair to raise the question about the relevance of these results to the function of mammalian lung surfactant with a more complex composition and operating at higher temperatures. There are three relevant parameters conditioning the nanostructure of the film: molecular composition, surface pressure, and temperature. Although the conditions for the three parameters used in the experiments reported here do not exactly reproduce the physiological ones, the main conclusion refers to the effect of the presence of the SP-B protein on the nanostructure of the film and, subsequently, on its mechanical stability. We strongly believe that this conclusion can be extrapolated to other conditions where domains are present in the film, even if the parameters originating them are somewhat different. Pulmonary surfactant films of complex composition, containing all the protein and lipid complement, show LE/LC coexistence domains and lateral segregation at pressures above 35 mN/m (Nag et al., 1998; Discher et al., 1996), at both room temperature and 37°C. Mechanisms originating those film patterns probably include not only pressure-driven LE-LC transitions but also segregation of different components into nonmiscible phases with distinct molecular organization. Pure DPPC or the DPPC/DPPG films studied here show LE/LC coexistence plateaus at around 11 mN/m at 25°C. To test whether the effect of SP-B on the microstructure of DPPC/DPPG was temperature dependent, we ran pilot experiments at 37°C. At this temperature, the LE/LC plateau is reached when the films are compressed beyond 24 mN/m. At 37°C and this pressure range, pure DPPC/DPPG films show the same coexistence of condensed microdomains and nanodomains seen here at 11 mN/m and 25°C (not shown). Furthermore, presence of SP-B caused the same qualitative effects on decreasing the apparent condensation and modifying the nanoscopic morphology as seen in this work, suggesting that SP-B could have an analogous structural effect on the ordered/disordered coexistence pattern shown by pulmonary surfactant films at physiologically relevant conditions. Experiments at 37°C, however, have multiple technical problems, including subphase evaporation, bubble formation, and thermal disequilibration between liquid, air, and solid supports, all preventing a precise quantitative analysis.

Two-dimensional aggregation of SP-B

SFM also suggests that SP-B can induce formation of aggregates that are associated with the borders of liquid-

condensed DPPC or DPPC/DPPG domains. These aggregates, presumably of SP-B, may consist of two-dimensional clusters of SP-B molecules. The size and number of these clusters are proportional to the protein content of the lipid/protein film and do not change significantly with compression. The frictional properties of these aggregates are different from those of any other region of the films, including LE or LC lipid domains. Association of these presumed protein clusters with the borders of condensed DPPC domains resembles the appearance of other protein aggregates (Reichert et al., 1992; Ruano et al., 1998), reinforcing the idea that these boundaries can behave as sinks of immiscible monolayer ''impurities.'' We had previously detected accumulation of surfactant SP-A surrounding the domain boundaries of DPPC (Ruano et al., 1998, 1999), and also of SP-C (unpublished results), using fluorescently labeled proteins. It could be possible that the LE phase of DPPC or DPPC/DPPG would dissolve much less protein in the absence of NBD-PC, where more than 90% of its surface is actually condensed, than in the presence of the probe, favoring the segregation of protein clusters we see by SFM. We detect formation of protein clusters at protein/lipid percents as low as 2% (w/w). The physiological content of SP-B in native surfactant, around 1% by weight, could then be close to the ''solubility limit'' of the DPPC expanded phase. However, the presence in surfactant of other lipid components different than DPPC or DPPG, such as unsaturated PC and PG species or cholesterol, could also influence solubility and lateral distribution of the protein in both the air-liquid interface and the LB supports. Studies in this regard are in progress.

The protein clusters associated at the boundaries of the DPPC condensed domains are not simple, amorphous aggregates but have a defined thickness of 4–6Å. This feature suggests that the clusters might consist of two-dimensional aggregates of protein molecules, one molecule thick.

This study is an example of how SFM of lipid/protein films transferred from the air-liquid interface to solid supports can provide detailed information on the architecture of pulmonary surfactant films at different compressions which are relevant for respiratory dynamics. The study of the behavior and the morphology of the complete set of surfactant lipids and proteins will further help to understand their complex interrelationships.

We are indebted to Professor Hans-Joachim Galla from University of Münster (Germany) and Professor H. William Taeusch from University of California San Francisco for their comments and useful suggestions and the critical reading of the manuscript.

This work has been supported by grants from Dirección General de Educación Superior e Investigación Científica (BIO2000-0929 and BIO2003-09056) and Comunidad Autónoma de Madrid (08.2/0054/2001.1). A.C. was recipient of a postdoctoral fellowship from Comunidad Autónoma de Madrid.

REFERENCES

Bangham, A. D., C. J. Morley, and M. C. Phillips. 1979. The physical properties of an effective lung surfactant. *Biochim. Biophys. Acta.* 573:552–556.

Clark, J. C., S. E. Wert, C. J. Bachurski, M. T. Stahlman, B. R. Stripp, T. E. Weaver, and J. A. Whitsett. 1995. Targeted disruption of the surfactant protein B gene disrupts surfactant homeostasis, causing respiratory failure in newborn mice. *Proc. Natl. Acad. Sci. USA.* 92:7794–7798.

Cruz, A., C. Casals, K. M. Keough, and J. Perez-Gil. 1997. Different modes of interaction of pulmonary surfactant protein SP-B in phosphatidylcholine bilayers. *Biochem. J.* 327:133–138.

Cruz, A., C. Casals, and J. Perez-Gil. 1995. Conformational flexibility of pulmonary surfactant proteins SP-B and SP-C, studied in aqueous organic solvents. *Biochim. Biophys. Acta.* 1255:68–76.

Cruz, A., C. Casals, I. Plasencia, D. Marsh, and J. Perez-Gil. 1998. Depth profiles of pulmonary surfactant protein B in phosphatidylcholine bilayers, studied by fluorescence and electron spin resonance spectroscopy. *Biochemistry.* 37:9488–9496.

Cruz, A., L. A. Worthman, A. G. Serrano, C. Casals, K. M. Keough, and J. Perez-Gil. 2000. Microstructure and dynamic surface properties of surfactant protein SP-B/dipalmitoylphosphatidylcholine interfacial films spread from lipid-protein bilayers. *Eur. Biophys. J.* 29:204–213.

Deleu, M., M. Paquot, P. Jacques, P. Thonart, Y. Adriaensen, and Y. F. Dufrene. 1999. Nanometer scale organization of mixed surfactin/phosphatidylcholine monolayers. *Biophys. J.* 77:2304–2310.

Diemel, R. V., M. M. Snel, A. J. Waring, F. J. Walther, L. M. van Golde, G. Putz, H. P. Haagsman, and J. J. Batenburg. 2002. Multilayer formation upon compression of surfactant monolayers depends on protein concentration as well as lipid composition. An atomic force microscopy study. *J. Biol. Chem.* 277:21179–21188.

Ding, J., D. Y. Takamoto, A. von Nahmen, M. M. Lipp, K. Y. Lee, A. J. Waring, and J. A. Zasadzinski. 2001. Effects of lung surfactant proteins, SP-B and SP-C, and palmitic acid on monolayer stability. *Biophys. J.* 80:2262–2272.

Discher, B. M., K. M. Maloney, W. R. Schief, Jr., D. W. Grainger, V. Vogel, and S. B. Hall. 1996. Lateral phase separation in interfacial films of pulmonary surfactant. *Biophys. J.* 71:2583–2590.

Discher, B. M., W. R. Schief, V. Vogel, and S. B. Hall. 1999. Phase separation in monolayers of pulmonary surfactant phospholipids at the air-water interface: composition and structure. *Biophys. J.* 77:2051–2061.

Feder, J. 1988. Fractals. Plenum Press, New York.

Frerking, I., A. Gunther, W. Seeger, and U. Pison. 2001. Pulmonary surfactant: functions, abnormalities and therapeutic options. *Intensive Care Med.* 27:1699–1717.

Goerke, J. 1998. Pulmonary surfactant: functions and molecular composition. *Biochim. Biophys. Acta.* 1408:79–89.

Goerke, J., and J. Gonzales. 1981. Temperature dependence of dipalmitoyl phosphatidylcholine monolayer stability. *J. Appl. Physiol.* 51:1108–1114.

Grunder, R., P. Gehr, H. Bachofen, S. Schurch, and H. Siegenthaler. 1999. Structures of surfactant films: a scanning force microscopy study. *Eur. Respir. J.* 14:1290–1296.

Hawgood, S., M. Derrick, and F. Poulain. 1998. Structure and properties of surfactant protein B. *Biochim. Biophys. Acta.* 1408:150–160.

Hollars, C. W., and R. C. Dunn. 1998. Submicron structure in L-alpha-dipalmitoylphosphatidylcholine monolayers and bilayers probed with confocal, atomic force, and near- field microscopy. *Biophys. J.* 75:342–353.

Johansson, J., T. Curstedt, and B. Robertson. 2001. Artificial surfactants based on analogues of SP-B and SP-C. *Pediatr. Pathol. Mol. Med.* 20:501–518.

Knebel, D., M. Sieber, R. Reichelt, H. J. Galla, and M. Amrein. 2002a. Fluorescence light microscopy of pulmonary surfactant at the air-water interface of an air bubble of adjustable size. *Biophys. J.* 83:547–555.

Knebel, D., M. Sieber, R. Reichelt, H. J. Galla, and M. Amrein. 2002b. Scanning force microscopy at the air-water interface of an air bubble coated with pulmonary surfactant. *Biophys. J.* 82:474–480.

Kramer, A., A. Wintergalen, M. Sieber, H. J. Galla, M. Amrein, and R. Guckenberger. 2000. Distribution of the surfactant-associated protein C within a lung surfactant model film investigated by near-field optical microscopy. *Biophys. J.* 78:458–465.

Krol, S., M. Ross, M. Sieber, S. Kunneke, H. J. Galla, and A. Janshoff. 2000. Formation of three-dimensional protein-lipid aggregates in monolayer films induced by surfactant protein B. *Biophys. J.* 79:904–918.

Liepinsh, E., M. Andersson, J. M. Ruysschaert, and G. Otting. 1997. Saposin fold revealed by the NMR structure of NK-lysin. *Nat. Struct. Biol.* 4:793–795.

Lipp, M. M., K. Y. Lee, J. A. Zasadzinski, and A. J. Waring. 1996. Phase and morphology changes in lipid monolayers induced by SP-B protein and its amino-terminal peptide. *Science.* 273:1196–1199.

Mohwald, H. 1990. Phospholipid and phospholipid-protein monolayers at the air/water interface. *Annu. Rev. Phys. Chem.* 41:441–476.

Morrow, M. R., J. Perez-Gil, G. Simatos, C. Boland, J. Stewart, D. Absolom, V. Sarin, and K. M. Keough. 1993. Pulmonary surfactant-associated protein SP-B has little effect on acyl chains in dipalmitoylphosphatidylcholine dispersions. *Biochemistry.* 32:4397–4402.

Nag, K., C. Boland, N. Rich, and K. M. Keough. 1991. Epifluorescence microscopic observation of monolayers of dipalmitoylphosphatidylcholine: dependence of domain size on compression rates. *Biochim. Biophys. Acta.* 1068:157–160.

Nag, K., J. G. Munro, S. A. Hearn, J. Rasmusson, N. O. Petersen, and F. Possmayer. 1999a. Correlated atomic force and transmission electron microscopy of nanotubular structures in pulmonary surfactant. *J. Struct. Biol.* 126:1–15.

Nag, K., J. G. Munro, K. Inchley, S. Schurch, N. O. Petersen, and F. Possmayer. 1999b. SP-B refining of pulmonary surfactant phospholipid films. *Am. J. Physiol.* 277:L1179–L1189.

Nag, K., J. Perez-Gil, A. Cruz, and K. M. Keough. 1996. Fluorescently labeled pulmonary surfactant protein C in spread phospholipid monolayers. *Biophys. J.* 71:246–256.

Nag, K., J. Perez-Gil, M. L. Ruano, L. A. Worthman, J. Stewart, C. Casals, and K. M. Keough. 1998. Phase transitions in films of lung surfactant at the air-water interface. *Biophys. J.* 74:2983–2995.

Nag, K., S. G. Taneva, J. Perez-Gil, A. Cruz, and K. M. Keough. 1997. Combinations of fluorescently labeled pulmonary surfactant proteins SP-B and SP-C in phospholipid films. *Biophys. J.* 72:2638–2650.

Nielsen, L. K., T. Bjornholm, and O. G. Mouritsen. 2000a. Fluctuations caught in the act. *Nature.* 404:352.

Nielsen, L. K., A. Vishnyakov, K. Jorgensen, T. Bjornholm, and O. G. Mouritsen. 2000b. Nanometer-scale structure of fluid lipid membranes. *J. Phys.: Condens. Matt.* 12:A309–A314.

Nogee, L. M., G. Garnier, H. C. Dietz, L. Singer, A. M. Murphy, D. E. deMello, and H. R. Colten. 1994. A mutation in the surfactant protein B gene responsible for fatal neonatal respiratory disease in multiple kindreds. *J. Clin. Invest.* 93:1860–1863.

Pastrana-Rios, B., C. R. Flach, J. W. Brauner, A. J. Mautone, and R. Mendelsohn. 1994. A direct test of the ''squeeze-out'' hypothesis of lung surfactant function. External reflection FT-IR at the air/water interface. *Biochemistry.* 33:5121–5127.

Perez-Gil, J. 2001. Lipid-protein interactions of hydrophobic proteins SP-B and SP-C in lung surfactant assembly and dynamics. *Pediatr. Pathol. Mol. Med.* 20:445–469.

Perez-Gil, J. 2002. Molecular interactions in pulmonary surfactant films. *Biol. Neonate.* 81 (Suppl 1):6–15.

Perez-Gil, J., C. Casals, and D. Marsh. 1995. Interactions of hydrophobic lung surfactant proteins SP-B and SP-C with dipalmitoylphosphatidylcholine and dipalmitoylphosphatidylglycerol bilayers studied by electron spin resonance spectroscopy. *Biochemistry.* 34:3964–3971.

Perez-Gil, J., A. Cruz, and C. Casals. 1993. Solubility of hydrophobic surfactant proteins in organic solvent/water mixtures. Structural studies on SP-B and SP-C in aqueous organic solvents and lipids. *Biochim. Biophys. Acta.* 1168:261–270.

Perez-Gil, J., and K. M. Keough. 1998. Interfacial properties of surfactant proteins. *Biochim. Biophys. Acta.* 1408:203–217.

Perez-Gil, J., K. Nag, S. Taneva, and K. M. Keough. 1992. Pulmonary surfactant protein SP-C causes packing rearrangements of dipalmitoylphosphatidylcholine in spread monolayers. *Biophys. J.* 63:197–204.

Piknova, B., W. R. Schief, V. Vogel, B. M. Discher, and S. B. Hall. 2001. Discrepancy between phase behavior of lung surfactant phospholipids and the classical model of surfactant function. *Biophys. J.* 81:2172–2180.

Reichert, A., H. Ringsdorf, and A. Wagenknecht. 1992. Spontaneous domain formation of phospholipase A2 at interfaces: fluorescence microscopy of the interaction of phospholipase A2 with mixed monolayers of lecithin, lysolecithin and fatty acid. *Biochim. Biophys. Acta.* 1106:178–188.

Reiter, G. 1992. Dewetting of thin polymer films. *Phys. Rev. Lett.* 68: 75–78.

Ross, M., S. Krol, A. Janshoff, and H. J. Galla. 2002. Kinetics of phospholipid insertion into monolayers containing the lung surfactant proteins SP-B or SP-C. *Eur. Biophys. J.* 31:52–61.

Ruano, M. L., K. Nag, C. Casals, J. Perez-Gil, and K. M. Keough. 1999. Interactions of pulmonary surfactant protein A with phospholipid monolayers change with pH. *Biophys. J.* 77:1469–1476.

Ruano, M. L., K. Nag, L. A. Worthman, C. Casals, J. Perez-Gil, and K. M. Keough. 1998. Differential partitioning of pulmonary surfactant protein SP-A into regions of monolayers of dipalmitoylphosphatidylcholine and dipalmitoylphosphatidylcholine/dipalmitoylphosphatidylglycerol. *Biophys. J.* 74:1101–1109.

Schram, V., and S. B. Hall. 2001. Thermodynamic effects of the hydrophobic surfactant proteins on the early adsorption of pulmonary surfactant. *Biophys. J.* 81:1536–1546.

Shiffer, K., S. Hawgood, H. P. Haagsman, B. Benson, J. A. Clements, and J. Goerke. 1993. Lung surfactant proteins, SP-B and SP-C, alter the thermodynamic properties of phospholipid membranes: a differential calorimetry study. *Biochemistry.* 32:590–597.

Shih, W. H., W. Y. Shih, S. I. Kim, J. Liu, and I. A. Aksay. 1990. Scaling behavior of the elastic properties of colloidal gels. *Phys. Rev. A.* 42: 4772–4779.

Shiku, H., and R. C. Dunn. 1998. Direct observation of DPPC phase domain motion on mica surfaces under conditions of high relative humidity. *J. Phys. Chem. B.* 102:3791–3797.

Takamoto, D. Y., M. M. Lipp, A. von Nahmen, K. Y. Lee, A. J. Waring, and J. A. Zasadzinski. 2001. Interaction of lung surfactant proteins with anionic phospholipids. *Biophys. J.* 81:153–169.

Taneva, S., and K. M. Keough. 1994. Pulmonary surfactant proteins SP-B and SP-C in spread monolayers at the air-water interface: I. Monolayers of pulmonary surfactant protein SP-B and phospholipids. *Biophys. J.* 66:1137–1148.

Vandenbussche, G., A. Clercx, M. Clercx, T. Curstedt, J. Johansson, H. Jornvall, and J. M. Ruysschaert. 1992. Secondary structure and orientation of the surfactant protein SP-B in a lipid environment. A Fourier transform infrared spectroscopy study. *Biochemistry.* 31:9169–9176.

Veldhuizen, E. J., J. J. Batenburg, L. M. van Golde, and H. P. Haagsman. 2000. The role of surfactant proteins in DPPC enrichment of surface films. *Biophys. J.* 79:3164–3171.

Weaver, T. E. 1998. Synthesis, processing and secretion of surfactant proteins B and C. *Biochim. Biophys. Acta.* 1408:173–179.

Weaver, T. E., and J. J. Conkright. 2001. Function of surfactant proteins B and C. *Annu. Rev. Physiol.* 63:555–578.

Yu, S. H., and F. Possmayer. 1996. Effect of pulmonary surfactant protein A and neutral lipid on accretion and organization of dipalmitoylphosphatidylcholine in surface films. *J. Lipid Res.* 37:1278–1288.